Material-related issues at high-power and high-energy ion beam facilities

M. Bender[1*], D. Severin[1], M. Tomut[1] and C. Trautmann[1,2]

[1]GSI Helmholtzzentrum, Planckstr. 1, 64291 Darmstadt, Germany
[2]Technische Universität Darmstadt, Alarich-Weiss-Str. 2, 64287 Darmstadt, Germany

E-mail: m.bender@gsi.de

Abstract. When solids are exposed to energetic ions (MeV-GeV), their physical and chemical structure can be severely modified. The change is governed by ultrafast dynamical processes starting from the deposition of large energy densities, electronic excitation and ionization processes, and finally damage creation in the atomic lattice system. In many materials, each projectile creates a cylindrical track with a few nanometers in diameter and up to many μm in length. To study and monitor the creation of damage, the GSI irradiation facility dedicated to materials science provides different in-situ and on-line techniques such as high resolution microscopy, X-ray diffraction, optical absorption spectroscopy, thermal imaging and residual gas analysis. The irradiation experiments can be performed under various gas atmospheres and under cryogenic or elevated temperature.

1. Introduction

When heavy ions above a specific energy of some 100 keV/u penetrate solids they mainly excite the electronic subsystem of the target [1]. On a time scale of 10^{-17} s, delta electrons are created that spread the energy radially around the trajectory of the projectile [2]. The following electron cascade distributes the energy inside of the electronic system within a time scale of up to 10^{-14} s. During this period, the atomic lattice is still cold. The redistributed electrons lead to a high space charge resulting in Coulomb repulsion of the ionized atoms, if the electrons do not compensate the space charge fast enough. After 10^{-13} - 10^{-12} s, the electrons transfer their energy to the atom subsystem due to electron-phonon-coupling leading to ultrafast heating of the lattice. Temperatures exceeding melting or vaporization of the target can be reached. Depending on the target material, this thermal spike may last up to 10^{-10} s. If the subsequent cooling of the liquefied cylinder along the ion path is rapid enough, quenching of atomic disorder occurs and a so-called ion track is formed. Track formation is pronounced in insulators such as polymers, ionic crystals, oxides as well as few III-V semiconductors and selected metallic alloys, but most pure metals and pure Si and Ge do not show track formation [3].

The track consists of a cylindrical zone of damaged material and has a typical diameter of several nanometers [4]. Tracks in particular in polymers can be selectively attacked by a suitable chemical etchant converting the damage trail into an open pore. The fact that each heavy ion produces an individual track which exhibits preferential etchability is the base of the ion-track nanotechnology. With this technique, small but extremely long (up to several tens of μm) channels can be fabricated. Their diameter is very uniform and can be adjusted by the etching process between about 10-20 nm and several μm. Track-etched membranes are available

as commercial products and are applied in many different fields, e.g., as special filters, cell cultivation substrates, or as templates for the synthesis of micro- and nanowires [3, 5].
While individual ion tracks are utilized as nanostructures, the integral action of many overlapping tracks may lead to macroscopic changes and severe radiation damage. Damage effects are of particular concern for materials and devices exposed to high-intensity ion beams at the new high-power accelerators such as CERN and the future facility for antiproton and heavy ion research (FAIR). The existing GSI accelerator and the upcoming FAIR facility comprise several "hot spots" where materials face extreme radiation levels, e.g., stripper foils at the UNILAC, the future production target for the Super Fragment Separator (SFRS) and beam catchers [6]. Although they consist of carbon-based materials of rather high radiation hardness, the expected high beam intensities will result in structural and mechanical damage, requiring cost and time intensive maintenance. Of special concern are also organic insulating materials because under extensive beam exposure they embrittle and become conductive, a risk for magnet insulation and other electrical devices.
Another material-related issue is the deterioration of the vacuum of the accelerator system leading to enhanced beam losses. If the beam hits the inner surface of the beamline, the impacts of energetic ions initiate the release of gas [7, 8, 9]. Especially for high-intensity beams such as at the future synchrotron SIS100 at FAIR or at the S3 beamline of SPIRAL 2 (Caen, France), the amount of desorbed gas may be enormous, rendering beam-induced molecular desorption a critical issue for next generation accelerators. In the following, we provide a short description of the GSI irradiation facilities dedicated to materials research and ion beam induced effects. Selected examples of FAIR-relevant material issues including radiation hardness of specific components and desorption phenomena are presented.

2. Irradiation facilities for materials research

At the existing GSI facility, several beam lines are dedicated to materials research including target handling, beam monitoring and various online and in-situ analytical methods. The linear accelerator UNILAC provides all ion species up to uranium with energies up to 11.4 MeV/u where the typical range of the ions is about 100 μm. The X0-beamline is equipped with an automated sample exchange system for the efficient irradiation of up to 100 samples per hour. The beam is defocused in such a way that an area of 5 x 5 cm^2 is homogeneously illuminated. Applied fluences range from one single ion per sample to about 10^{13} ions/cm^2. Using the heavy-ion microprobe [10], single ions can be placed on a predefined position within a lateral accuracy of better than 1 μm. This microbeam allows radiation hardness tests of selected areas of electronic devices. For biophysics experiments, single ions are shot into the nuclei of living biologic cells allowing monitoring of protein processes responsible for repairing the radiation damage. The M-Branch comprises three different beamlines dedicated to high-fluence irradiations (up to $\sim 10^{14}$ ions/cm^2) combined with online and/or in-situ analysis of beam-induced materials modifications. At the M1-beamline [11] a scanning electron microscope (including an EDX system) and an atomic force microscope (under UHV condition) is installed. The M2-beamline houses an x-ray diffractometer suitable for monitoring beam-induced structural changes or amorphization of a sample. The M3-beamline is equipped with a large universal irradiation chamber to which various spectrometers [12] (e.g., Fourier transform infrared (FTIR) and Raman), a residual gas analyser (RGA), thermal camera, as well as resistivity or mechanical creep test equipment can be attached. The samples can be irradiated at temperatures between 15 K and almost 1000° C. A scheme of the M3 beamline is shown in figure 1.
The heavy-ion synchrotron SIS-18 delivers beams with much higher energies up to several 100 MeV/u into cave A. At such high energies the corresponding ion ranges are up to cm, thus the irradiation of bulk samples is possible. Besides radiation hardness tests of mm to cm thick samples or devices, materials research activities also concentrate on the irradiation of samples

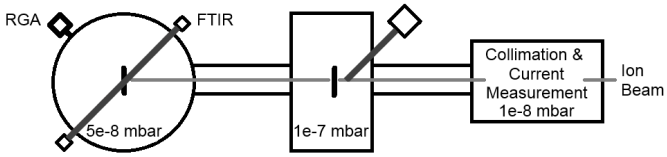

Figure 1. Schematic view of M3-beamline. The ion beam passes a diagnostic and collimation system (right) before entering the irradiation chamber. In the middle chamber, high temperature irradiation can be performed and the samples can be monitored with a thermal camera. In the left chamber, samples can be irradiated at cryogenic temperatures and various online spectroscopy techniques (e.g., FTIR or UV-vis) can be attached.

exposed to high pressures [16, 17, 18]. For this, miniaturized samples are mounted in diamond anvil cells which allow the generation of several tens of GPa. The cells are composed of two opposing 2-3 mm thick facetted diamonds which are squeezed together. Between the diamonds a gasket with a hole contains the sample in a pressure medium. The SIS-18 beam reaches the sample after penetrating the first diamond. The simultaneous exposure to pressure and radiation provides the possibility to simulate extreme conditions as present in the Earth mantle [4]. In the future also heating of the diamond anvil cell by a laser system is foreseen.

3. Ion-induced desorption

The release of gas into the vacuum system, triggered by impinging ions is a critical issue concerning beam losses and was investigated in the past at GSI and CERN [13]. For room temperature targets, the amount of desorbed gas per projectile ion (defined by the desorption yield η) scales with $(\mathrm{dE/dx})^2$ and can be described by a pure surface process, whereas the thermodynamic behavior of the substrate plays an important role for the release. In the above described thermal spike process, the ion impact leads to a region of elevated temperature resulting in enhanced thermal desorption. Several experiments with different beams and targets provided desorption yields which are in good quantitative agreement with thermal-spike model calculations [14].

Desorption effects are of concern when highest beam intensities are involved, e.g., at the SPIRAL-2 accelerator that will deliver some 10^{14} ions per second on a production target for rare isotopes. Even if the desorption yield is low, the high beam current will lead to enormous gas loads in the range of 10^{-3} mbar L s^{-1}. To the production target special rods are attached which stop the primary beam upon separating the rare isotopes. For thermal reasons the rods have to be made from a high melting material such as tungsten. The desorption yields of three different W samples were measured at the M1-beamline at GSI. For the irradiation 4.8 MeV/u Au ions with charge states 26+ and 53+ and respective currents of 3e-9 A and 3e-10 A were used. The pulse rate was 2 Hz and the pulse length 1.2 ms. The beam spot had a diameter of 6 mm. Two of the samples stem from the same batch of original rod material. They were brazed onto a Cu block as thermal substrate. The sample thickness was 3 mm which is much larger than the projected range of the Au projectiles (~ 17 μm). The third sample was cut from a pure W foil of 50 μm thickness. All samples were mounted on holders that could be inserted into the beam. The base pressure in the irradiation chamber was 1.8 e-8 mbar. During beam exposure, the dynamic vacuum, i.e., the total and partial pressures were recorded.

Figure 2 presents the results of the total desorption yield as a function of the accumulated fluence (left) and the partial pressure evolution for the thin W target irradiated with Au^{26+} ions (right). The yields were calculated from the pressure increase inside the vacuum chamber during irradiation. The overall uncertainty is estimated to be around 30% due to the large errors of

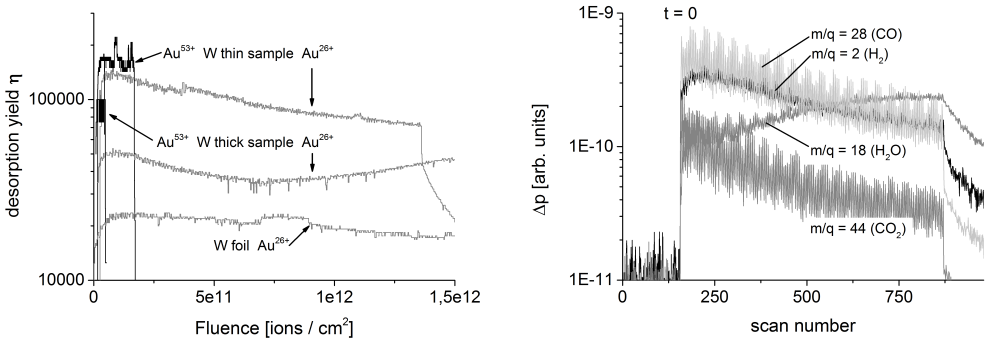

Figure 2. Left: desorption yields (released gas molecules per incident ion) for different W samples, measured with 4.8 MeV/u Au^{26+} and Au^{53+} ions. Right: partial pressure rise for the most relevant gas components. Irradiation starts at t = 0 and ends at scan number 875, corresponding to a fluence of 1.5e12 ions per cm^2.

the pressure and pumping speed measurements. Note that the beam current for the 53+ beam was one order of magnitude less than for the 26+ beam. Hence, within a fixed beamtime, much less fluence is accumulated. For a given sample, the higher charge state leads to higher desorption yields due to the higher energy loss of the 53+ beam [14]. The desorption yield tends to slightly decrease with increasing fluence due to beam scrubbing (cleaning of the surface with the ion beam). However, there are other effects which may increase the desorption yield (see m/q = 18 in Fig. 2 right). After the irradiation, the corresponding thick sample contained many macroscopic cracks where gas could be released under beam exposure. The composition of the desorbed gas is predominately H, CO and CO_2 (see Fig. 2, right) as observed so far for any sample and beam condition. The desorption yields measured for these tungsten samples are surprisingly high compared to earlier measurements using Au or Cu targets [15].

4. Radiation hardness of carbon-based materials

Graphite and other carbon based materials are the main choice for targets and beam protection parts facing intense primary beams. Their response to beam-induced thermal stress and stress waves is by far more favorable than standard materials such as stainless steel, due to their superior thermo-mechanical properties.

To test beam-induced damage processes and radiation hardness limits, thin carbon foils for electron stripping and bulk graphite as target for the production of secondary beams were irradiated with U and Au ions of 4.8 MeV/u kinetic energy. The beam was delivered from the high current source with a repetition rate of 1 - 2 Hz and pulse length of about 100 μs. This low duty cycle is leading to an enormous instantaneous power density deposition of 10 MW/g per pulse. For online investigation of beam-induced materials modifications, the infrared transmittance and radiance of 20 $\mu g/cm^2$ thin amorphous foils were monitored with the FTIR spectrometer and a fast thermal camera of type FLIR SC7500. This infrared camera is able to record fully radiometric images with kHz repetition rate and can be synchronized to the beam pulse. Therefore, the spatial and time decay of the heat load from the ion beam on the sample can be recorded with high precision and gives input for simulations of stress wave propagation. Figure 3 shows the thermography of a graphite foil exposed to a collimated U beam recorded at the maximum intensity of the beam pulse (left) and the evolution of the maximum temperature in the beam spot as a function of time (right).

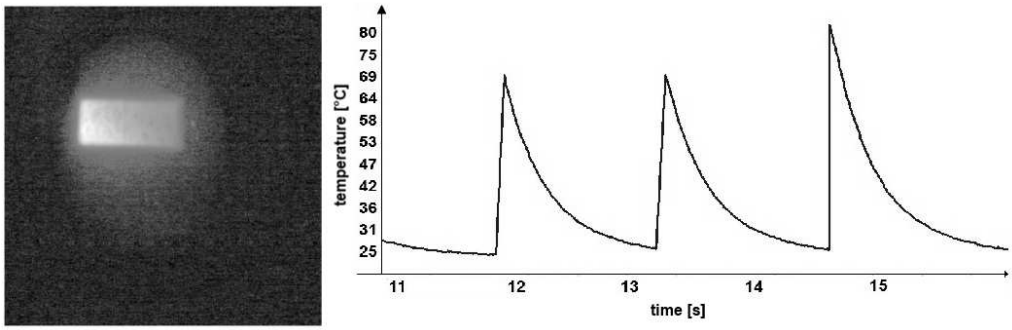

Figure 3. Left: Radiometric image of a graphite foil sample during irradiation with a low duty cycle 4.8 MeV/u U^{238} ion beam with a repetition rate of 0.6 Hz and a beam pulse duration of 150 μs. Image size is $\approx$ 5 x 5 cm^2. Temperature is coded in brightness. In this plot, bright colors within the rectangular beam spot are corresponding to temperatures higher than 40 °C, at the maximum intensity of the beam pulse. Right: maximum temperature within the beam spot versus time. The spikes correspond to individual ion beam pulses.

5. Conclusion and Outlook

Ion-induced molecular desorption from surfaces and radiation hardness of materials are important issues for FAIR and other next generation heavy-ion accelerators. At present, these processes are only partially understood and more detailed investigations are needed in particular for those accelerator components and devices that will be exposed to high-power and high-energy ion beams. Various analytical online systems allow the monitoring of radiation effects as a function of irradiation dose including processes such as material degradation, structural changes, outgassing, and temperature increase of the samples. The knowledge gain on damage creation is mandatory for limiting aging processes and providing life time estimates for safe device operation.

At the new FAIR facility, the BIOMAT beamline of the APPA cave will offer possibilities for irradiating samples at multiple extreme conditions including temperature, pressure and particularly high intensity irradiation not available at the existing SIS facility.

We acknowledge the support of FP7 EuCARD-2 under grant agreement no. 312453.

[1] Siegmund P. 2006 *Mat. Fys. Med.* **52-2** 557
[2] Toulemonde M., Assman W., Dufour C., et al. 2006 *Mat. Fys Med.* **52-2** 263
[3] Trautmann C. 2009 in *Ion Beams in Nanoscience and Technology* 369
[4] Lang M. Lian J., Zhang F. , et al. 2008 *Earth and Planetary Science Letters* **274** 355
[5] Toimil-Molares M. E. 2012 *Beilstein J. Nanotechnol* **3** 860
[6] Geissel H., Weick H., Winkler M., et al. 2003 *Nucl. Instr. Meth.* **B 204** 71
[7] Calder R. S. 1974 *Vacuum* **24** 437
[8] Mahner E., Hansen J., Küchler D., et al. 2002 *Proc. EPAC* 2568
[9] Zhang S. Y. and Ahrens L. A. 1999 *Proc. PAC* 3294
[10] Fischer B. and Heiss M. 2007 *Nucl. Instr. Meth.* **B 260** 442
[11] Amirthapandian S., Schuchart F. and Bolse W. 2010 *Rev. Sci. Inst.* **81** 033702
[12] Baake O., Seidl T., Hossain, U. H., et al. 2011 *Rev. Sci. Inst.* **82** 045103
[13] Mahner E., Hansen J., Laurent, J.-M., et al. 2003 *Phys. Rev. ST-AB* **6** 013201
[14] Bender M., Kollmus H., Reich-Sprenger H., et al. 2009 *Nucl. Instr. Meth.* **B 267** 885
[15] Bender M., Kollmus H. and Assmann W., et al. 2007 *Nucl. Instr. Meth.* **B 256** 387
[16] Lang M., Zhang F., Lian J., et al. 2009 *J. Synch. Rad.* **16** 773
[17] Schuster B., Lang M., Klein R., et al. 2009 *Nucl. Instr. Meth.*. **267** 964
[18] Glasmacher U. A., Lang M., Keppler H., et al. 2006 *Phys. Rev. Lett.* **96** 195701